Study of electrical relaxation mechanism of TiO$_2$ doped Bi-polymer systems

Moumita Khutia[1], Girish M. Joshi[1*], Subhratanu Bhattacharya[2]

[1]*Polymer Nanocomposite Laboratory, Material Physics Division, School of Advanced Sciences,*
VIT University, Vellore 632014, Tamil Nadu, India
[2]*Department of Physics, University of Kalyani, Nadia 741235, West Bengal, India*

*Corresponding author. Tel: (+91) 9894566487; E-mail: varadgm@gmail.com

ABSTRACT

Polyvinyl alcohol (PVA) /Poly (tetrafluoroethylene) (PTFE)/Titanium oxide (TiO$_2$) was prepared by (5, 10 and 15 wt %) TiO$_2$ loading. The miscibility, thermal property and microstructure of the composites were characterized by differential scanning calorimetry (DSC) and scanning electron microscopy (SEM). The electrical relaxation dynamics including dielectric and electrical conductivity was examined as a function broadband of frequency and temperature. The dielectric data was analyzed via the electric modulus. The Maxwell-Wagner-Siller (MWS) effect corresponds to interfacial polarization at low frequency follows Arrhenius behavior. The α-mode relaxation is attributed to glass-rubbery transition in composites, obeys the Vogel- Taman-Fulcher (VTF) model. A slight bump was noted at relatively high temperature and high frequencies termed as Intermediate dipolar effect (IDE) obeys the Arrhenius behavior. Conductive mechanism was analyzed via AC conductivity spectra. However, DC conductivity follows Arrhenius equation. The overall studies confirm that the self relaxation mechanism of PVA/PTFE composites were modified by TiO$_2$ offers the tuning conductivity as a function of the temperature which can be used in various electronic applications. Copyright © 2016 VBRI Press.

Keywords: Polymer composite; titanium oxide; dielectric relaxation; conductivity.

Introduction

The ceramic metal oxide based polymer nanocomposites has created huge interest among the scientific community due to their outstanding performance in electronic properties since a decade [1, 2]. Generally ceramic materials are brittle in nature and very difficult to process [3]. On the other hand, polymer materials are pliable and easy to process at low temperature. It exhibits very high dielectric breakdown fields [4]. The mixture of two interdependent polymers and ceramic materials in the composite structure exhibits high electrical performance. However, the electrical properties such as conductivity, dielectric constant, loss can be optimized by loading, type and quantity of ceramic oxide. Titanium dioxide (TiO$_2$) is very well known transition metal oxide which can be subjected in many studies due to its excellent optical and electronic properties [5]. It has three distinct crystallization structures such as rutile, anatase and brookite [6]. Generally nano size TiO$_2$ exhibits modified physical and chemical properties in compare with the bulk structure. Due to inexpensive, good thermal stability, nontoxic nature, best photo catalytic property with wide band gap was preferred for the photocatalytic and device applications [7, 8]. The applications of TiO$_2$ mostly depend on size (nano), structure and morphology which effect on the performance and properties [9].

Poly (tetrafluoroethylene) (PTFE) is a hydrophobic polymer exhibiting the unique thermal and chemical resistance, low surface friction and excellent fracture toughness. Focusing on the exceptional combination, PTFE becomes a prime material for industrial filters, membrane applications [10]. Standard PTFE has very high molecular mass (10^7 g/mole) with very high melt viscosity (10^{11} Pa.s) [11]. Furthermore, PTFE cannot dissolve in any organic solvent. Therefore, many patents disclosed various methods like extruder to build expanded PTFE film [12, 13]. The great challenges for casting the PTFE require high processing temperature and very difficult to control micron size uniform thickness of film. However, very few investigations have been reported on PTFE blend and composite preparation using PTFE emulation.

PVA is nontoxic, hydrophilic semi-crystalline polymer with wide range of applications in medical and technology [14]. The blending of PTFE with PVA is expected to increase the chemical and mechanical properties of PVA system. The formation of hydrogen bond between PVA and PTFE segment could promote the miscibility of PVA and PTFE. Huang *et al.* investigated the effect of mass ratios (from 1:1 to 4:1) of PTFE emulsion and PVA matrix on the morphologies and the properties of membrane [15]. The mass ratio increases the membrane roughness and porosity from 23.2 to 38.6 (wt %). The chemical constitution and thermal degradation of PVA/PTFE composite membrane, before and after sintering exhibit no significant changes [16]. The uniqueness of this bi-polymer composite membrane has strong thermal stability and good hydrophobicity, anticorrosive and environmental friendly. It demonstrates best surface barrier property which may be used to tailor high performance engineering composite.

In the present era of polymer physics domain, the research based on polymer composites are generally focused to optimized the electrical property. Different types of methods such as blending, co polymerization and addition of ceramic filler are used for development of composites. The polymer composites are heterogeneous system with one or two polymer systems and required to adjust the desired filler. This modified version of blends exhibit better electrical performance as function of filler. The charge carriers are accumulated by the displacements and reorientation of dipoles under external a.c. electric field. This effect is called interfacial polarization which is followed by Maxwell- Wagner- Siller (MWS) theory. Generally the conduction mechanism and the dipolar effect of the polymer composite materials can be investigated by the electrical relaxation mechanism. The dielectric permittivity, electrical modulus spectra, impedance and conductivity spectra were used to investigate the electrical relaxation formalism [17]. Modulus formalism is the easiest method to study the electrical relaxation of mono, multi polymer systems [6].

However, in the present study we motivated to prepare the PVA/PTFE/TiO$_2$ composites and study the electrical relaxation behavior as a function of frequency and temperature. The samples were characterized by DSC, SEM to investigate the effect of filler on structure, thermal property and morphology.

Experimental

Material details

PVA graduals of grade RS-2117 (MW=124000 g/mole) was made by Kuraray Exceval, Japan procured from by Associate Agencies, Mumbai. The commercial product PTFE concentrated suspension of grade INOFLON AD9300 was supplied by Gujarat Fluoro chemicals Ltd (GFL). The emulsion contains 60 wt % of solid of PTFE. The average particle size of PTFE is 0.21 μm. The filler nano TiO$_2$ of grade AEROXIDE, P2 with specific surface 50 ± 15 m^2/ g, was supplied by Degussa, Germany. The particle size of TiO$_2$ is 21 nm with 80 % anatase and 20 % rutile structure.

Preparation of PVA/PTFE/TiO$_2$ composite

The pure and 5, 10 and 15 wt % TiO$_2$ loaded PVA/PTFE composite were prepared by solution casting. Initially the PVA solution was prepared by dissolving PVA granules in distilled water at 60 °C under constant stirring (410 rpm for 1hr). Upon cooling at room temperature (35 °C), the dispersed PTFE emulsion was added to the PVA solution and stirred (410 rpm for 2 hrs) to get the homogeneous PVA/PTFE solution blending. Then, the sample was cast into the petri dish at room temperature (35 °C) and covered by aluminum foil. After 48 hrs the PVA/PTFE blend was peeled off and use for further characterization.

We modified PVA/PTFE by loading of TiO$_2$ (5, 10 and 15 wt %). The TiO$_2$ nano powder was sonicated in distilled water (30 mins) by ultrasonic tab at room temperature (35 °C) until its homogeneous dispersion. After that dispersed TiO$_2$ was added into PVA/PTFE emulsion and stirred (410 rpm for 2 hrs) by maintaining the same experimental conditions. Then solution was poured in the clean, dry petri dish at room temperature. After (48 hrs) the PVA/PTFE/TiO$_2$ composite film has been obtained and used for further characterization.

Characterization

DSC measurements were carried out by NETZSCH, STA-449 calorimeter in standard mode with nitrogen gas purging at the rate of 20 ml/min. Approximately 10 mg sample was used for DSC measurement. The Samples were heated to 300 °C at the rate of 10 °C / min. The recording has been done in heating process.

The morphologies of the samples were recorded by Zeiss Scanning electron microscope (SEM) to ascertain the surface morphology of samples for various TiO$_2$ loading. The samples were stained with gold metal.

The electrical characterizations of the composites were characterized by N-4L, PSM 1735 impedance analyzer. The sample dimension with thickness 120-130 μm and diameter 13 mm, was kept in the fixer with ALAB BTC 9100 temperature controller across the broadband frequency range 50 Hz-10 MHZ and temperature range 40 °C -110 °C.
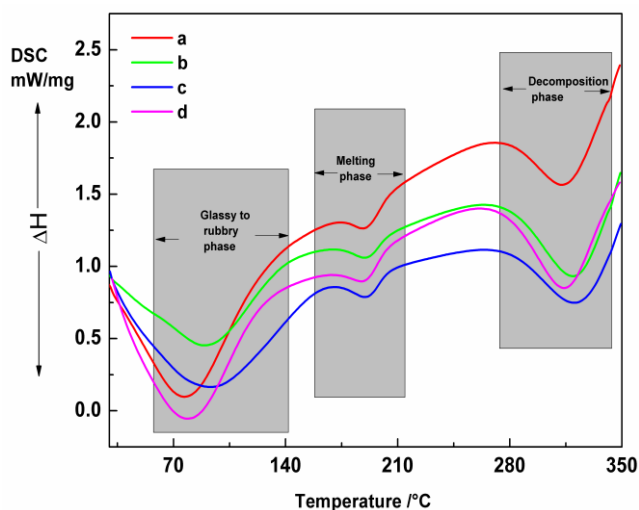

Fig. 1. DSC thermogram of (a) 0, (b) 5, (c) 10 and (d) 15 wt % TiO$_2$ loaded PVA/PTFE composites designated with varying phases.

Results and discussion

DSC analysis

DSC analysis is the one of the important thermal analysis, which is used to interpret the thermal transition in the polymer blends and composites under heating and cooling process at uniform flow of nitrogen. The glass transition temperature (T$_g$), melting temperature (T$_m$) and decomposition temperature (T$_d$) can be analyzed by this technique. The DSC thermogram of (0, 5, 10, 15 wt %) TiO$_2$ loaded PVA/PTFE composite are shown in (**Fig. 1(a-d)**) with temperature (30-350 °C). The peak at 76 °C corresponds to the thermal effect due to glass transition (**Fig. 1a**). The single T$_g$ value are found evaluated DSC thermogram, which indicates the miscibility of two polymers. The T$_g$ and T$_m$ value of pure PVA is 88.1 °C and 209.6 °C, which is already reported [18]. The

broad peak at glass transition depends on OH composition [18]. The 5 wt % TiO_2 loaded PVA/PTFE composite shows highest T_g (**Fig. 1b**). The OH groups of PVA are interconnected with TiO_2 and PTFE which corresponds to high T_g. It decreases with TiO_2 loading (**Fig. 1c, d**). The endothermic peak of pure PVA/PTFE at 189.48 ^{0} C corresponds to the T_m with enthalpy 52.82 J/g. The decrease of enthalpy and T_m suggests that the loading of TiO_2 affects the crystallinity which shows decreasing magnitude as function of TiO_2. The thermal fusion for 100 % crystalline PVA is 138.60 J/g **[19]**. The formula to calculate crystallinity of polymer is defined underneath **[20]**.

$$X_C = \frac{\Delta H_m(T_m)}{\Delta H_m^0(T_m^0)} \%$$
(1)

where, $\Delta H_m(T_m)$ is the thermal fusion at melting temperature T_m, and $\Delta H_m^0(T_m^0)$ is the thermal fusion of 100 % crystalline PVA at T_m^0.

Table I. Values of T_g, T_m, T_d, enthalpy at melting point and degrees of crystallinity of pure and TiO_2 loaded PVA/PTFE composites.

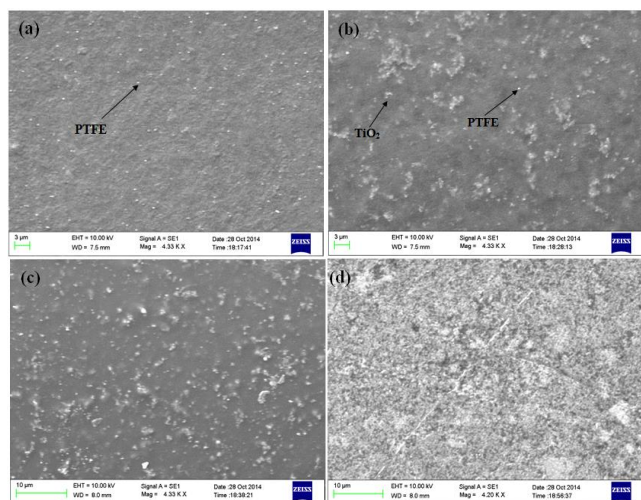| Samples	T_g (^{0}C)	T_m ^{0}C)	T_d (^{0}C)	Enthalpy (J/g)	Crystallinity (X_c) (%)
PVA/ PTFE	76	189	313	52.82	37.5
5 wt% TiO_2	89	188	318	46.3	33.1
10wt % TiO_2	88	186	320	37.25	26.7
15wt % TiO_2	78	187	319	38.9	27.4

Fig. 2. The SEM micrograph of (a) 0, (b) 5, (c) 10 and (d) 15 wt % TiO_2 loaded PVA/PTFE composites.

The T_g, T_m, Heat fusion due to T_m, and the degrees of crystallinity is tabulated in **Table I**. The crystallinity value of pure PVA/PTFE, calculated from DSC curve is about 37.5 %. The reorientation of polymer chain may be arise by cross linking centered formed by interaction between PVA, PTFE, with TiO_2. As a result the degree of crystallization decreases with TiO_2 content. The addition of TiO_2 in PVA, PTFE is responsible to enhance segmental chain motion of polymer which can enhance DC conductivity. At 15 wt % TiO_2 loaded PVA/PTFE composite, crystallinity increases slightly due to filler aggregation. This also reduces corresponding DC conductivity. Another endothermic crystalline peak has been appearing at 313 ^{0}C which

corresponds to decomposition temperature **[21]**. Usually the decomposition is take place in pure PVA from 200 ^{o}C and the majority of mass loss is observed in between 230-330 ^{o}C **[22]**. The values of T_d increase up to 10 wt % TiO_2 loading. For 15 wt % TiO_2 loading, T_d decreases which confirms that the thermal stability of the composite reduces due to filler aggregation.

SEM analysis

SEM micrograph of 0, 5, 10, 15 wt % TiO_2 loaded composites are shown in (**Fig. 2(a-d)**). No micro pores were found in any of the composites. **Fig. 2a** does not reflect the crystallite behavior at the given magnification. The distribution of PTFE on PVA matrix is shown clearly. For the low amount of TiO_2 loading, exhibit the heterogeneous micro-structure of the modified blend shown in the (**Fig. 2(b-c)**). It can be observed that TiO_2 are nano size. The distribution of TiO_2 on PVA/PTFE is almost symmetric. In **Fig. 2d**, the certain aggregation of TiO_2 nanoparticles are also found. The system with TiO_2 particle interface shows good interaction between PTFE, PVA and TiO_2.

Electrical analysis

In polymer composite, the electrical relaxation phenomena could include the contribution from both polymer (PVA, PTFE) and ceramic filler (TiO_2). The respective dielectric responses are including interfacial polarization (MWS), which are expected to occur at low frequency due to filler effect and α-relaxation, which are arising at transition point of glassy and rubbery state **[23]**. The recorded dielectric parameter could be first express in terms of the real (ε′) and imaginary part (ε″) of dielectric permittivity. The calculated dielectric permittivity was transformed into electrical modulus formalism via Eq. 2. The advantage of using electrical modulus formalism is that it can easily interpret the bulk relaxation properties. The variation of dielectric permittivity and conductivity is lower at low frequency which is the main drawback to distinguish the relaxation peaks **[24]**. The complex electrical modulus can be defined as the inverse of complex electrical permittivity **[25]**.

$$M^* = \frac{1}{\varepsilon^*} = \frac{1}{\varepsilon' - j\varepsilon''} = \frac{\varepsilon'}{\varepsilon'^2 + \varepsilon''^2} + j\frac{\varepsilon''}{\varepsilon'^2 + \varepsilon''^2} = M' + jM''$$
(2)

where, M′ and M′′ are the real and imaginary part of electrical modulus.

This formalism includes the phenomena of electrode polarization and space charge effect which leads to high values of permittivity and conductivity at low frequencies and high temperature. The resulting benefit of electrical modulus has been reported **[25, 26]**. The plot of ε′ (left Y-axis) and M′ (right Y-axis) versus frequency of 0, 5, 10 and 10 wt % TiO_2 loaded PVA/PTFE composite is shown in **Fig. 3a-d** in log- log representation at temperature range 40-110 ^{0}C. The high ε′ value at low frequency for pure and TiO_2 loaded PVA/PTFE composites can be also explained by MWS effect **[23]**.
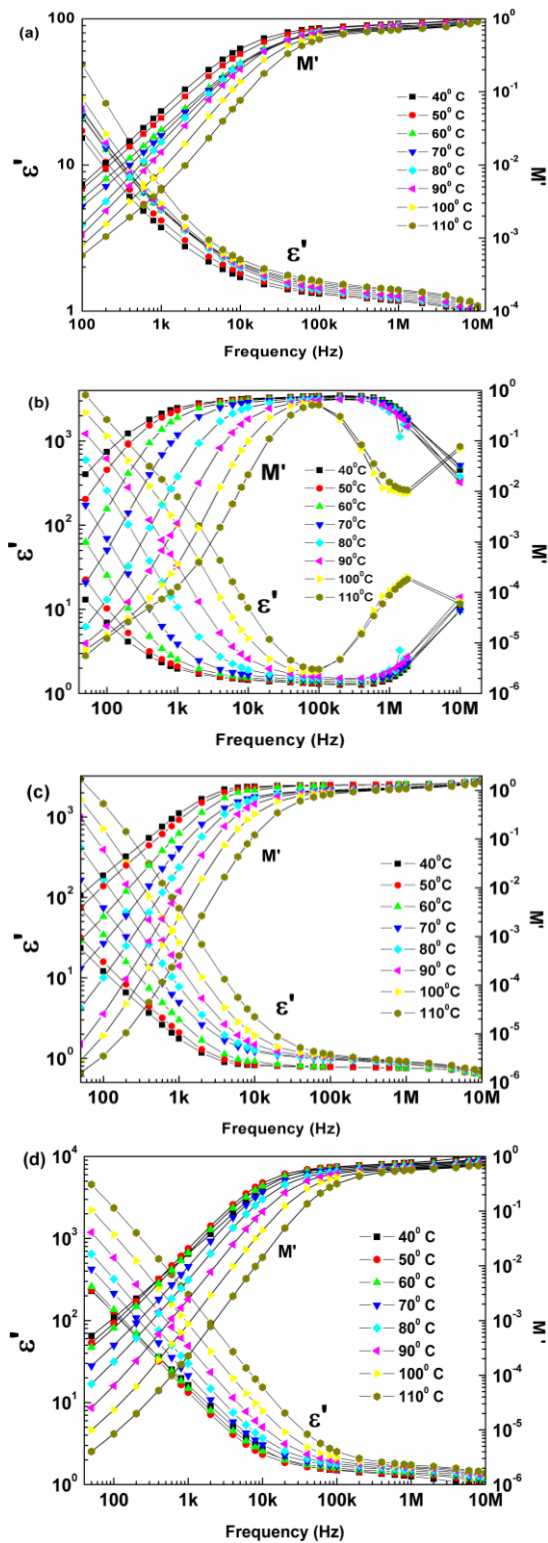
Fig. 3. The real part of dielectric permittivity (ε′) (left Y axis) and electrical modulus (M′) (right Y-axis) of (a) 0, (b) 5, (c) 10 and (d)15 wt % TiO$_2$ loaded PVA/PTFE composites.

Fig. 4a-d, the plot of ε″ (left Y-axis) and M″ (right Y-axis) versus frequency of 0, 5, 10 and 15 wt % TiO$_2$ loaded PVA/PTFE composite is depicted in log-log representation.
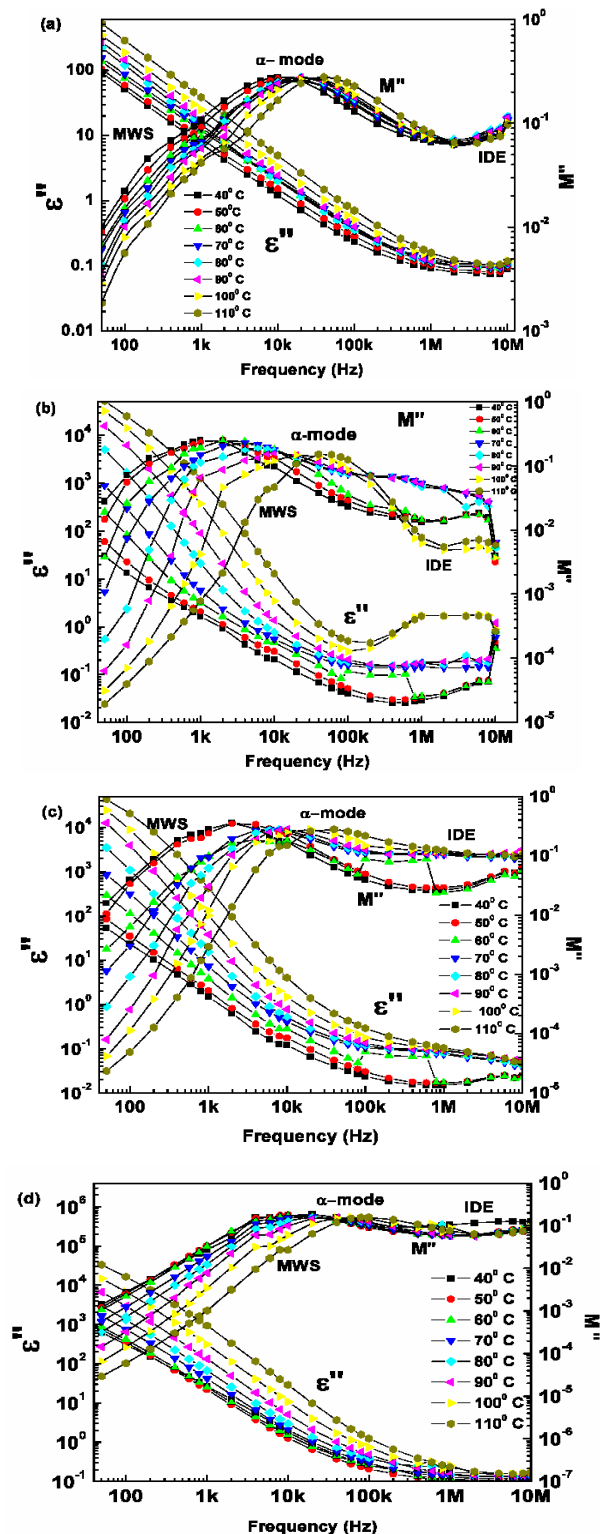

Fig. 4. The imaginary part of dielectric permittivity (ε′′) and electrical modulus (M′′) of (a) 0, (b) 5, (c) 10 and (d) 15 wt % TiO$_2$ loaded PVA/PTFE composites.

At the polymer/filler interface, the charges are accumulated and create large dipole. These dipoles are not able to align properly with the AC electric field [24, 25]. The composite system are consisting wide band gap semiconductor TiO$_2$ and insulating PTFE, PVA polymer increases dielectric permittivity with TiO$_2$ loading. In

At low frequency one very weak interaction is detected at the shoulder of M" versus frequency plot at any given

temperature. The interfacial polarization or MWS is responsible for the occurrence of this mode [**6, 24**]. The MWS is the one type of relaxation process which appears at the heterogeneous system due to charge carrier accumulation at the interfaces of systems. When temperature is increased the gradual increase of ε' and ε'' occurs. This phenomenon is the result of two competing mechanism: one is segmental motion of polymer chain which increases with temperature and another is thermal expansion of polymer [**22**]. However, near glass transition temperature the segmental motion of polymer causes large effect in dielectric permittivity. Another broad relaxation peak known as α-mode represents a relaxation process which has been accompanied by loss peak in the diagram of M'' versus frequency. This is related to the glass- rubber transition of the polymer [**27**]. The peak position is shifted towards higher frequencies with increasing temperature. The magnitude and shape of the peak position has been shifted slowly from 40-80 ^{0}C. Above 80 ^{0}C, the magnitude of the peak and shifting rate also increased. The MWS relaxation exhibits high electrical heterogeneity between their phases at higher loading (**Fig. 4b-d**). The α-mode relaxation peak shifted towards lower frequency for 5 wt % TiO$_2$ loaded PVA/PTFE with respect to pure PVA/PTFE. The α-mode is more pronounced in higher loading of TiO$_2$ (**Fig. 4b-d**).
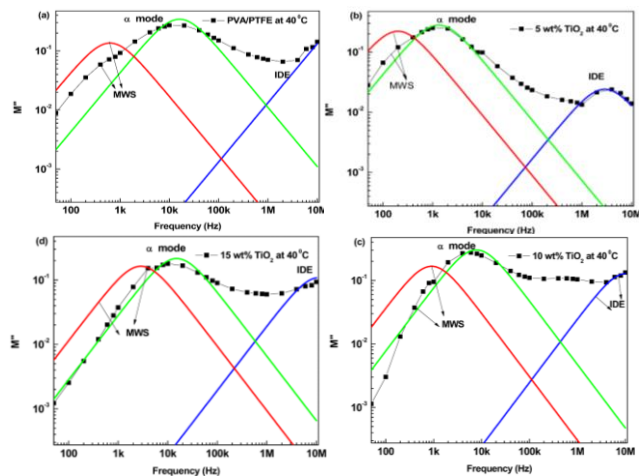
Fig. 5. The fitting of (a) 0, (b) 5 (c) 10 and (d) 15 wt% TiO$_2$ loaded bi polymer system at 40 ^{0}C. The experimental data was fitted by three Debye process (MWS, α-mode and IDE-mode)**.**

The intensity of the peak also varies with filler content. Thus the appearance of the relaxation is highly affected with filler concentration. The intermediate dielectric spectra is situated between the slow (MWS and α-mode) and fast (local mode) process. This can be termed as Intermediate dipolar effect (IDE) [**6, 24, 28**]. The IDE mode become sharper at 5 and 10 wt % TiO$_2$ loaded PVA/PTFE. For 15 wt % TiO$_2$ loaded PVA/PTFE, the IDE effect become less. The physical origin of IDE effect cannot be described distinctly. The TiO$_2$ is a polar oxide which exhibits transition in crystal structure with varying symmetry. The structure of TiO$_2$ is 80 % anatase and 20 % rutile. The low unit cell symmetry of TiO$_2$ with tetragonal structure indicated strong polarization is occurring in PVA/PTFE/TiO$_2$ composite. The influence of temperature

on the distance sites of TiO$_2$ could effect on structure which affect the redistribution of polarization [**6**]. The electrical relaxation for single relaxation time in terms of dielectric modulus can be expressed as:

$$M' = M_s M_\infty \frac{M_\infty + M_s \omega^2 t^2}{M_\infty^2 + M_s^2 \omega^2 t^2} \qquad (3)$$

$$M'' = M_s M_\infty \frac{(M_\infty - M_s)\omega t}{M_\infty^2 + M_s^2 \omega^2 t^2} \qquad (4)$$

The above equations are known as Debye's dispersion. To interpret three relaxation process in PVA/PTFE/TiO$_2$ composites, we have fitted M'' versus frequency plot by Eq. 4 using multi peak fitting. For an example, the fitting procedure of all TiO$_2$ loaded PVA/PTFE composite at 40 ^{0}C is shown in **Fig. 5**.
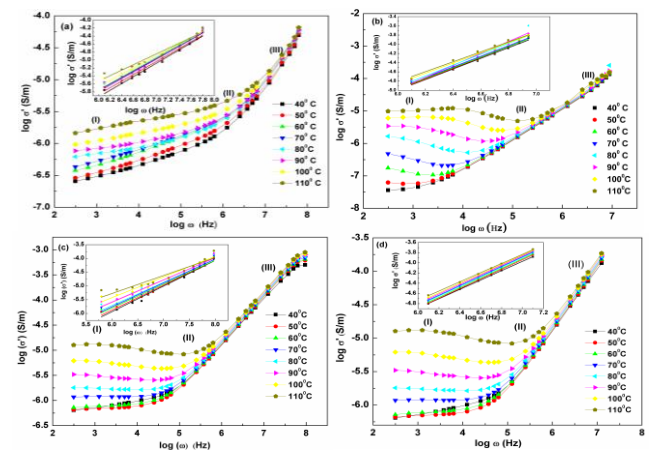
Fig. 6. The real of AC conductivity (σ´) versus frequency for (a) 0, (b) 5, (c) 10 and (d) 15 wt % TiO$_2$ loaded PVA/PTFE composites at temperature range 40-110^0 C. The top inset of each plot shows the best fit of AC conductivity with power law approach.

The experimental points are described by solid fitted line of superposition of Debye type relaxation (MWS, α-mode and IDE mode). The Debye type relaxations contain single relaxation time which was evaluated by fitting parameters. The evaluated relaxation times are correlated as a function of filler loading and effectively pronounced in α and IDE mode. From the fitting parameters, the three types of relaxations were demonstrated as frequency relaxation and temperature dependent criteria. The *M''* peaks is shifted towards higher frequency with the increasing temperature (**Fig. 4a-d**) due to the frequency temperature superposition. The peak shift rate differs for different relaxation process (MWS, α-mode and IDE).

The real and imaginary parts of Alternating Current (AC) conductivity, σ' and σ'' was calculated from Eq. 5 and 6 [**29**].

$$\sigma' = \varepsilon_0 \omega \varepsilon'' \qquad (5)$$

$$\sigma'' = \varepsilon_0 \omega \varepsilon'' \qquad (6)$$

where, ε$_0$= 8.85x10^{-12} F/m is the permittivity of free space. Real part of AC conductivity as a function of frequency is presented in **Fig. 6** at temperature range 40-110 ^{0}C for 0, 5, 10 and 15 wt % TiO$_2$ loaded PVA/ PTFE composites. An increase of conductivity with temperature is observed for

all tested samples. The frequency dependent AC conductivity can be divided into three distinct regions which indicate the existence of dissipated effects. At low frequency region (I) a leveled electrical conductivity is observed which corresponds to the DC conductivity of the samples.
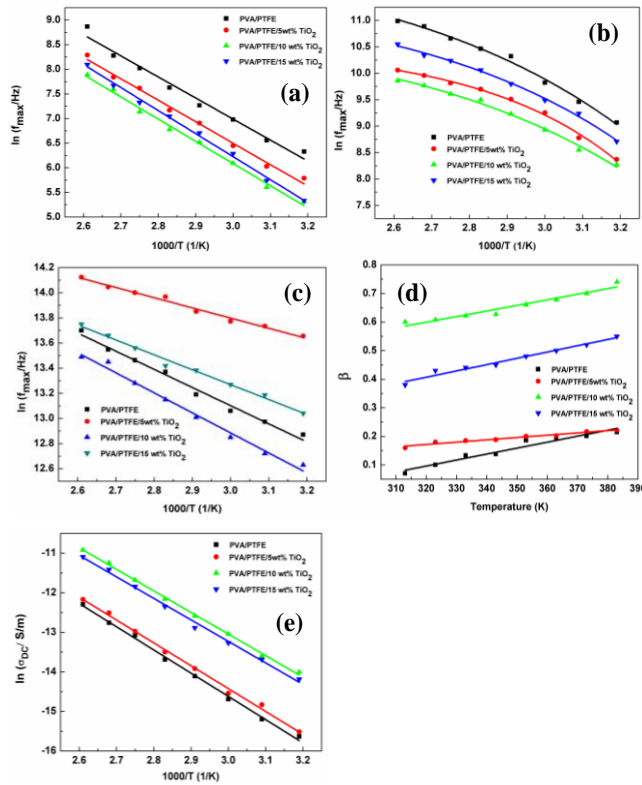

Fig. 7. Dependence of relaxation frequencies as a function of reciprocal temperature for (a) MWS relaxation, (b) α mode relaxation, (c) IDE relaxation process (d) β versus T (e) Arrhenius plot for conduction process.

It increases significantly as a function of the temperature. In the intermediate region (II) the dipolar relaxation is observed depending upon the filler content. At high frequency region (III) the conductivity increases with the increases of frequency following the Jonscher power law is shown by the following relations [30].

$$\sigma' = A\omega^s \tag{7}$$

where, is the power factors which are very close to value 1. The power factor s has been calculated from the slop of linear fitting of log σ' vs log ω at high frequency region (III). In the present case the observed behavior of s can be analyzed from the correlated barrier hopping (CBH) model. According to this model, the conduction of TiO_2 loaded PVA/PTFE occurs through bipolaron hopping process. The barrier height correlates with the intrinsic separation between the charges of columbic interaction. The frequency exponent s can be expressed as below [21, 31].

$$s = \frac{\log \sigma'}{\log \omega} = 1 - \frac{6k_B T}{W_m} \tag{8}$$

Or

$$1 - s = \frac{6k_B T}{W_m} = \beta \tag{9}$$

where, W_m is the barrier height, k_B is Boltzmann's constant; T is the temperature in Kelvin scale.

The DC conductivity has been evaluated by extrapolating the AC conductivity spectra at zero frequency. The temperature dependent DC conductivity values of all composites follows Arrhenius model is shown by following equation [32].

$$\sigma_{DC} = \sigma_0 \exp\left(-\frac{E_A}{k_B T}\right) \tag{10}$$

where, σ_0 is the pre exponential factor, E_A is the activation energy, k_B is the Boltzmann constant and T is the absolute temperature. The DC conductivity increases with up to 10 wt% TiO_2 loading. For 15 wt % TiO_2 loaded PVA/PTFE composite, DC conductivity decreases slightly. This suggests that the segmental motion of polymer chain has been dominated by the aggregation of TiO_2.

Fig. 7a-c represents the temperature dependence frequency relaxation rate for MWS, α-mode, IDE mode and DC conductivity. **Fig. 7(d, e)** represents β versus T and Arrhenius plot of conduction process of all tested samples. In the present case the MWS and IDE mode follows Arrhenius type behavior, described below [6].

$$f_{max} = f_0 \exp\left(-\frac{E_A}{k_B T}\right) \tag{11}$$

Or

$$\ln(f_{max}) = \ln f_0 - \left(\frac{E_A}{k_B T}\right) \tag{12}$$

where, E_A is activation energy , f_0 is the pre exponential factor, k_B is the Boltzmann constant and T is the absolute temperature. The peak shifting of α relaxation process is not constant and can be followed by Vogel-Tamann-Fulcher (VTF) equation [27].

$$f_{max} = f_0 \exp\left(-\frac{B}{T - T_0}\right) \tag{13}$$

Or

$$\ln(f_{max}) = \ln f_0 - \frac{B/T}{1 - T_0/T} \tag{14}$$

where, f_0 is the pre exponential factor, B is the constant to determine activation energy, T_0 is the Vogel temperature and T is the absolute temperature. The fitting parameter of MWS, α-mode and IDE mode via Eq. 12 and 14 of all tested sample were tabulated in **Table II**. It is found that the activation energy calculated from the MWS process increases with TiO_2 content. The increasing value of

activation energy with TiO$_2$ content indicates the heterogeneity. The maximum value of T$_0$ in α-mode corresponds to 5 wt % TiO$_2$ loaded PVA/PTFE composite and decreases accordingly with filler content. Finally, the parameter B decreases with filler content which indicates that, the required thermal energy for α- relaxation process decreases with TiO$_2$ concentration. The behavior indicates the existence of weak interaction between ceramic filler and PTFE, PVA.

Table II. Fitting parameters of Arrhenius equation for MWS process, IDE mode, DC conductivity, VTF equation of α-mode and barrier height of CBH model of all tested samples.

Samples	MWS model E$_A$ (eV)	T$_0$ (K)	α-mode B (K)	E$_A$ (eV)	IDE	DC conductivity E$_A$ (eV)	Barrier height W$_m$ (eV)
PVA/ PTFE	0.306	253	540	1.48	0.221	0.404	0.609
5 wt% TiO$_2$	0.318	260	693	1.925	0.215	0.578	0.599
10 wt% TiO$_2$	0.412	255	427	1.240	0.209	0.580	0.531
15 wt% TiO$_2$	0.529	252	248	0.7	0.213	0.587	0.553

The barrier height was calculated from the slope of the linear fitting and tabulated in **Table II**. The barrier height decreases up to 10 wt % TiO$_2$ loaded PVA/PTFE composite. At 15 wt % TiO$_2$ loaded PVA/PTFE composite, it increases slightly which may be due to aggregation of TiO$_2$.

The activation energy was calculated from the slope of the ln σ$_{DC}$ versus 1000/T graph which has been listed in **Table II**. It was seen that the temperature above T$_g$ the conduction process is much easier with low activation energy whereas the charge transport behavior at low temperature range corresponds to increase of thermal agitation at their own onset.

Conclusion

The PVA/PTFE/TiO$_2$ composites were prepared by solution casting. The influence of filler on T$_g$, T$_m$, T$_d$ and crystallinity of PVA/PTFE/TiO$_2$ composites were analyzed by DSC technique. It reveals that the crystallinity reduces with TiO$_2$ loading up to 10 wt % which confirms uniform dispersion of filler. At 15 wt % TiO$_2$ loading, the crystallinity increases slightly due to filler aggregation. SEM morphology confirms good presence of TiO$_2$ with bi-polymer system. The aggregation is also observed at 15 % TiO$_2$ loading. The dielectric relaxation confirmed by Debye electrical modulus equation. Three different relaxation are observed at MWS polarization, transition between glassy and rubbery state and the localize motion at polar side group. The glass transition temperature obtained from α- mode exhibits good correlation with DSC data. The shifting of T$_g$ with TiO$_2$ loading confirms the weak interaction between polymer chain and TiO$_2$. The activation energy co-related to all the relaxations peaks were calculated by using Arrhenius (MWS and IDE) and VTF (α-mode) models and inversely proportional to the TiO$_2$ loading. The strong variation of ac conductivity with frequency and temperature is observed in all the composites. The behavior of power factor obeys CBH model. The calculated barrier height from the power factor also depends on the wt % of TiO$_2$ loading. The DC conductivity is obtained by extrapolation of AC conductivity at zero frequency. It increases as a function of inverse of temperature following Arrhenius model. However, the presence of self relaxing polarization in the

TiO$_2$ loaded PVA/PTFE composite can be applicable for various electronic applications.

Reference

1. Qian, X.; Gu, N.; Yang, X.; Wang ,E.; Dong, S., *Electrochimica Acta,* **2001**,*46*, 1829.
    DOI: 10.1016/S0013-4686(00)00723-4
2. Chahal, P.; Tummala, R. R.; Allen M.G.; Swaminathan, M. *IEEE Transac. Comp. Packag. Manufac. Tech., Part B: Adv. Pack* **1998**, *21*, 184.
    DOI: 10.1109/96.673707
3. Y. Bai, Z. Y. Chang, V. Bharti, H.S. Xu and Q.M. Zhang, *Appl. Phy. Lett.,* **2000**, *76*, 3804.
    DOI: 10.1063/1.126787
4. Quan, H.; Chen, D.; Xie, X.; Fan, H., *Phys. Stat. Solidi.,* **2013**, *210*, 2706.
    DOI: 10.1002/pssa.201330234
5. Kovtyukhova, N.; Ollivier, P. J.; Chizhik, S.; Dubravin, A.; Bzaneva, E.; Gorchinskiy, A.; Marchenko A.; Smirnova, N., *Thin Solid Film.,* **1999**, *337*,166.
    DOI: 10.1016/S0040-6090(98)01197-3
6. Kontos, G. A.; Soulintzis, A. L.; Karahaliou, P.K.; Psarras, G.C.; Georga, S. N.; Krontiras C. A.; Pisanias, M.N., *Exp. Polym. Lett.* **2007**, *1*, 781.
    DOI: 10.3144/expresspolymlett.2007.108
7. Linsebigler, A.L.; Lu G.; Yates, J.T., *Chem. Rev.,* **1995**, *95*, 735.
    DOI: 10.1021/cr00035a013
8. Enachi, M.; Lupan, O.; Tudor Braniste,T.; Sarua,A.; Lee Chow, L.; Mishra, Y.K.; Gedamu, D.; Adelung,R.; Tiginyanu T., *Phys. Status Solidi, RRL- Rapid Res. Lett.,* **2015**, *9*, 171.
    DOI: 10.1002/pssr.201570615
9. Chakravadhanula, V. S. K.; Mishra, Y. K.; Kotnur V. G.; Avasthi, D. K.; Strunskus, T.; Zaporotchenko, V.; Fink,D.; Kienle, L.; Faupel, F., *Beilstein J. Nanotechnol.* **2014**, *5*, 1419.
    DOI:10.3762/bjnano.5.154
10. Tian, Z. Q.; Wang, X. L.; Zhang, H. M.; Yi B. L., Jiang, S.P. *Electrochem. Communic.,* **2006**, *8*, 1158.
    DOI: 10.1016/j.elecom.2006.05.011
11. Goessi, M.; Tervoort, T; Smith, P., *J. Mater. Sci.,* **2007**, *42*, 7983.
    DOI: 10.1007/s10853-006-1266-2
12. Newman, D.; Morizio, F.; Kidd, S., **2001,** *US patent* 6274043.
13. Arthur D. J.; Swei, G.S., **1991,** *US patent* 5024871.
14. Joshi, G. M.; Sharma, A.; Tibrawala, R.; Arora, S.; Deshmukh, K.; Kalainathan S.;Deshmukh, R. R., *Polym. Plast. Techn. Engin.,* **2014**, *53*, 588.
    DOI:10.1080/03602559.2013.854388
15. Huang, Q.; Xiao, C.; Hu X.; Li, X., *Desalination,* **2011**, *277*, 187.
    DOI: 10.1016/j.desal.2011.04.027
16. Huang, Q.; Xiao C.; Hu, X., *J. Mater. Sci.,* **2010**, *45*, 6569.
    DOI: 10.1007/s10853-010-4475-7
17. Ding, J.; Chen, S.C.; Wang X. L.; Wang, Y. Z., *Ind. Eng. Chem. Res.,* **2009**, *48*, 788.
    DOI: 10.1021/ie8013428
18. Guirguis O.W. Moselhy, M. T. H., *Natur. Sci.,* **2012**, *4*, 57.
    DOI: 10.4236/ns.2012.41009
19. Rault, J.; Gref, R.; Ping, Z. H.; Nguyen Q. T.; Neel, J., *Polymer* **1995**, *36*, 1551.
    DOI: 10.1016/0032-3861(95)99011-I
20. Polu, A. R.; Kumar, R., *Adv. Mater. Lett.,* **2013**, *4*, 543.
    DOI: 10.5185/amlett.2012.9417
21. Peppas, N. A.; Merril, E. W., *J. Appl Polym. Sci.,* **1976**, *20*, 1457.
    DOI: 10.1002/app.1976.070200604
22. Khutia, M.; Joshi, G.M.; Bhattacharya, S. *Ionics* **2015**.
    DOI: 10.1007/s11581-015-1500-5
23. Sharma, S.K.; Dutta, S.; Som, S.; Mandal, P.S., *J. Mater. Sci. Technol.,* **2013**, *29*, 633.

DOI: 10.1016/j.jmst.2013.03.014

24. Ramajo, L.A.; Cristobal, A. A.; Botta, P. M.; Porto Lopez , J. M.; Reboredo M. M.; Castro, M. S., *Composite: part A,* **2009**, *40*, 388.
    DOI: 10.1016/j.compositesa.2008.12.017

25. Psarras, G. C.; Manolakaki E.; Tsangaris, G. M., *Composite: Part A*, **2002**, *33*, 375.
    DOI: 10.1016/S1359-835X(01)00117-8

26. Psarras, G.C.; Manolakaki E.; Tsangarish, G. M., *Composite: Part A,* **2003**, *34*, 1187.
    DOI: 10.1016/S1359-835X(01)00117-8

27. Jin, X.; Zhang S.; Runt, J., *Macromolecules,* **2004**, *37*, 8110.
    DOI: 10.1021/ma049281b

28. Raptis, C. G.; Patsidis, A.; Psarras, G. C., *Exp. Polym. Lett.,* **2010**, *4*, 234.
    DOI: 10.3144/expresspolymlett.2010.30

29. Sahu, N.; Panigrahi S.; Kar, M., *J. Mater.,* **2013**, 802123.
    DOI: 10.1155/2013/802123

30. Shaaban M. H.; Ali, A. A., *J. Electro. Mater.,* **2013**, *42*, 1047.
    DOI: 10.1007/s11664-013-2512-4

31. G. C. Psarras, *Composite: Part A*, **2006**, *37*, 1545.
    DOI: 10.1016/j.compositesa.2005.11.004

32. Biswas, S.; Dutta, B.; Bhattacharya, S., *J. Mater. Sci.,* **2014**, *49*, 5910.
    DOI: 10.1007/s10853-014-8305-1

.